Infrared studies of hydrogenated amorphous carbon (*a*-C:H) and its alloys (*a*-C:H,N,F)

S. Liu and S. Gangopadhyay
Department of Physics, Texas Tech University, Lubbock, Texas 79409

G. Sreenivas, S. S. Ang, and H. A. Naseem
Department of Electrical Engineering, University of Arkansas, Fayetteville, Arkansas 72701
(Received 10 April 1996; revised manuscript received 15 October 1996)

We have used infrared (IR) absorption spectra to characterize *a*-C:H and its alloys (*a*-C:H,N,F). The samples were deposited in an rf plasma-enhanced chemical-vapor deposition system with various mixtures of CH_4, N_2, and NF_3 gases. IR spectra are analyzed in detail and the peak position assignments are based on the data published in the literature and calculation of the normal mode vibrational frequencies by assuming a simple force field and linear-molecular model. From IR analysis, we found that as the concentration of nitrogen and fluorine increases, the ratio of sp^2/sp^3 increases, while the hydrogen content decreases. The role of nitrogen is to break the symmetry and activate the olefinic C═C stretching mode. The role of fluorine is to replace hydrogen and to form stronger C—F bond. This explained the improvement of the thermal stability of electrical conductivity of *a*-C:H,N,F samples. [S0163-1829(97)04119-2]

I. INTRODUCTION

Hydrogenated amorphous carbon *a*-C:H films are of scientific interest because of their unusual structure and properties. *a*-C:H films exhibit extreme hardness, chemical inertness, optical transparency, good thermal conductivity, and good electrical insulation. These unique properties make *a*-C:H films ideal candidates for many applications, such as wear-resistant protective coatings for tools, as optical coatings, as protective coatings against corrosion, and as planarization layers for device fabrication.[1]

Doping of *a*-C:H films makes this material even more interesting. The effects of doping with boron, phosphorus, lithium, fluorine, and nitrogen have been studied by various groups.[2–4] Although light-emitting diodes based upon *a*-C:H active layers have already been realized,[5,6] the quantum efficiency of these devices is very low because the doping procedure has not been studied in detail. Recently, the effects of doping with nitrogen and fluorine on the growth and electrical properties of *a*-C:H have been extensively investigated by Sreenivas and co-workers.[7,8] They prepared polymerlike *a*-C:H films with an optical gap of 3.1 eV and above 50% hydrogen. Doping of these films with nitrogen and fluorine increased the refractive index, lowered the bulk resistivity, and lowered the optical band gap.[7,8] The most interesting property of the doped films was that they showed thermal stability up to 400 °C annealing temperature. The undoped polymerlike *a*-C:H films were converted to graphitic films at 200 °C annealing temperature. We have performed detailed infrared absorption measurements to understand the bonding configurations of various bonds and to understand the possible role of nitrogen and fluorine in these alloys.

II. EXPERIMENT

The deposition of *a*-C:H, *a*-C:H,N and *a*-C:H,N,F films was performed in a parallel-plate, capacitively coupled, 13.56 MHz Reinberg-type reactor (Texas Instruments Model A24C). An extensive discussion of the deposition procedure has been reported elsewhere.[7] Details of the deposition conditions are summarized in Table I.

Films grown on crystalline silicon and crystalline silicon coated with titanium tungsten (TiW) were used for Fourier transform infrared (FTIR) transmission and reflection measurements, respectively. The IR absorption spectra of the samples were recorded in a nitrogen ambient using a Perkin-Elmer FTIR spectrometer.

TABLE I. Processing parameters used to fabricate *a*-C H films and its alloys. Experimental conditions: deposition power (RF), 100 W (28 mW/cm^2); deposition frequency (RF), 13.56 MHz; deposition temperature, 100 °C; deposition time, up to 4 h; total gas pressure, 2 Torr. SCCM denotes cubic centimeter per minute at STP.

		Gas flow rates (SCCM)			
Sample	Thickness (Å)	CH_4	N_2	NF_3	Deposition rate (Å/min)
A	4000	200			19
B	4000	100	40		15
C	4000	200	200	20	22
D	4000	200		20	27

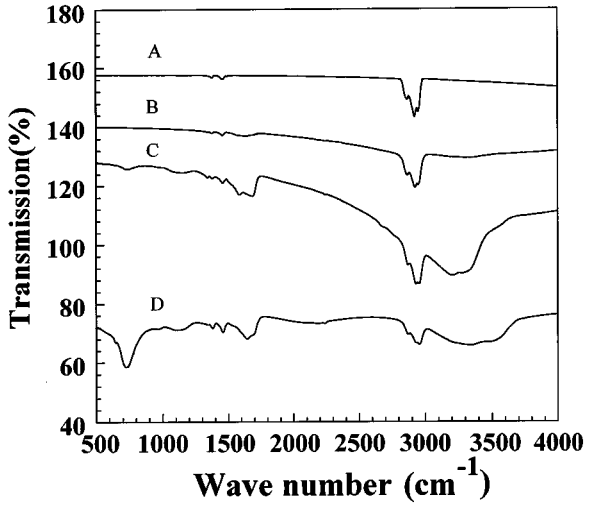

FIG. 1. Comparison of FTIR spectra of samples *A*, *B*, *C*, and *D*. The spectra are offset vertically for clarity.

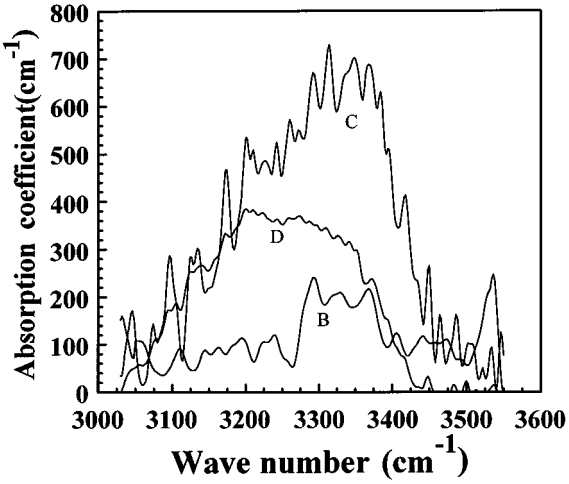

FIG. 2. IR absorption spectra around 3300 cm^{-1} for samples *B*, *C*, and *D*.

III. RESULTS AND DISCUSSION

The comparison of IR absorption of *a*-C:H films *A*–*D* in the range 500–4000 cm^{-1} is shown in Fig. 1. For clarity, the spectra are offset vertically. These spectra were taken in reflection mode.

From the IR spectra, some major features can be identified. The broad band around 3300 cm^{-1} is due to the NH_2 stretching mode.[9] The absorption peaks around 3000 cm^{-1} are due to CH stretching modes.[10] Their corresponding bending modes are observed around 1400 cm^{-1}. For nitrogen- and fluorine-doped samples, another feature around 2200 cm^{-1} shows up. This is the CN related mode.[7,9–11] Also a band around 1500–1750 cm^{-1} is observed for nitrogen- and fluorine-doped samples. In the lowest-energy region, only those samples containing fluorine show strong absorption, indicating that they are C-F related modes. Detailed and analyses are as follows.

A. Broad band around 3300 cm^{-1}

This band is due to the NH_2 stretching.[9] As expected, the IR spectrum of sample *A*, which does not contain nitrogen, is flat in this region. This band appears only when N_2 is added to the feed stock. Figure 2 shows the comparison of the absorption spectra of samples *B*, *C*, and *D*. The absorption spectrum was obtained by fitting the base line of the transmission spectrum (not shown) and then converting the transmission spectrum to absorption spectrum using the Beer-Lambert law. The transmission spectra were used in this region, because in the reflection spectra, it is difficult to fit the base lines for samples *C* and *D* in this region (see Fig. 1). As can be seen from Fig. 2, the absorption spectra obtained from the transmission spectra are very noisy. So for the other regions, only the reflection spectra were used to obtain absorption spectra. Sample *B* shows very weak absorption in 3300-cm^{-1} region and sample *C* has the strongest absorption. Because this band is well identified, a comparison of the absolute intensities of samples *B*, *C*, and *D* can be used to identify the NH_2 deformation band in the 1500–1750-cm^{-1} region, because the existence of many possible modes in this region makes the analysis difficult.

B. Band around 3000 cm^{-1}

The absorption peaks around 3000 cm^{-1} are due to CH stretching modes.[10] The integrated absorbances of this band can be used to estimate the hydrogen concentration in the film. It has been shown[12] that the concentration of the oscillating species is proportional to the integrated absorbances of the absorption band, i.e.,

$$N_{\mathrm{H}} = A \int \frac{\alpha(\omega)}{\omega}\, d\omega, \tag{1}$$

where N_{H} is the hydrogen atomic concentration, A is the proportionality factor, and $\alpha(\omega)$ is the absorption coefficient at frequency ω. For *a*-C:H films, A is chosen to be 1.35×10^{21} cm^{-2} from the work of Mui *et al.*[13] The calculated hydrogen concentrations of samples *A*–*D* are listed in Table II. Since our *a*-C:H film contains very high hydrogen concentration, it is polymerlike in nature. The incorporation of nitrogen or fluorine into the film decreases the hydrogen concentration.

The CH band consists of three peaks. The peak at 2956 cm^{-1} is due to sp^2-CH_2 (olefinic), the peak at 2920 cm^{-1} is due to the sp^3-CH_2 asymmetrical stretching mode, and the peak at 2870 cm^{-1} is due to the sp^3-CH_3 symmetrical stretching mode.[10] As can be seen in Fig. 1, the peak heights of these modes change with deposition conditions. To analyze the peak height change of these three peaks in more detail, we fitted the 3000 cm^{-1} band with three Gaussians. The peak positions and the area percentages calculated from the integrated absorbance are listed in Table II. In Table II, we have also listed the optical band gaps of these films obtained from optical absorption measurements using the Tauc equation.[14]

From this table it can be seen that the percentage of sp^2 species increases from 20.9% for film *A* to 44.2% for film *D*. It is well known that hydrogen incorporation in carbon films favors sp^3 bonding by etching sp^2 species.[15] As shown in Table I, the effect of nitrogen is to decrease the deposition rate. The reason is that the deposition of an *a*-CH film involves predominantly CH_3 and CH_3^+ species arriving at the

TABLE II. Summary of band gap, hydrogen contents, and sp^3 and sp^2 percentages of samples *A*, *B*, *C*, and *D*.

Sample	E_g (eV)	H content (%)	sp^3 CH_3 (sym.) (cm^{-1})	%	sp^3 CH_2 (asym.) (cm^{-1})	%	sp^2 CH_2 (ole.) (cm^{-1})	%
A	3.1	73.8	2863±0.7	37.1	2920±0.6	42.0	2955±0.5	20.9
B	2.9	67.3	2865±0.6	32.9	2919±0.7	37.4	2954±0.6	29.7
C	2.8	63.2	2870±0.5	28.9	2924±0.6	40.2	2959±0.7	30.9
D	2.6	57.4	2873±0.6	30.9	2921±0.5	24.9	2958±0.5	44.2

substrate surface. When the total deposition pressure is held constant at 2 Torr, introduction of N_2 in the feed stock results in the dilution of CH_3 radicals. Furthermore, when hydrogen is present, sp^2 content is increased because the hydrogen reacts with nitrogen and forms an amino group. The formation of nitrile (C≡N) groups is also favored over the formation of sp^3 species. Therefore, the addition of nitrogen to methane causes an increase in the sp^2/sp^3 ratio. The addition of NF_3 to the feed stock increases the deposition rate considerably. This is believed to be due to the reduction of activated hydrogen species by forming HF with the fluorine ions (F^-). Therefore, there is less atomic hydrogen to etch the graphitic carbon clusters. Thus the ratio of sp^2/sp^3 increases. Since the optical band gap depends primarily on the sp^2/sp^3 ratio,[16] a decrease in the band gap from samples *A*–*D* is expected (see Table II).

C. Band near 2200 cm^{-1}

The band near 2200 cm^{-1} also depends upon the deposition conditions. We observed two (for sample *B*) or three (for samples *C* and *D*) peaks in the 2150–2300 cm^{-1} range. When the film is deposited from pure CH_4 there is no feature in this region. When N_2 is added to the precursor gas, two peaks at 2180 and 2240 cm^{-1} show up indicating they are the CN-related modes. When NF_3 is added to the precursor gas(es) CH_4 (and N_2), another peak at 2210 cm^{-1} appears between these two peaks, suggesting that it is fluorine related. To get the exact peak positions, we fitted this band with two Gaussians for sample *B* and three Gaussians for samples *C* and *D*. The peak positions obtained from the best fit are 2182±5, 2211±3, and 2238±6 cm^{-1}. The fitted curves for samples *B*, *C*, and *D* are shown in Fig. 3. We assume a simple valence force field and linear-molecular model to calculate the vibrational frequencies of various possible compositions of molecules.[16] If we assume the force constants $F_{C\text{-}C}$=4.5 mdyn Å, $F_{C\equiv N}$=17.5 mdyn Å, $F_{C=N}$=11.7 mdyn Å,[17] and F_{C-N}=4.85 mdyn Å,[18] then the calculated in-phase stretching frequencies of molecules —C—C≡N, —N═C═N—, and F—N═C═N— are 2240, 2175, and 2200 cm^{-1}, respectively. Comparing with the observed values, we assigned the 2238 cm^{-1} peak to the stretching frequency of triple bonded —C≡N attached to the carbon network, the 2182 cm^{-1} peak to —N═C═N— stretch, and the 2211 cm^{-1} peak to fluorine attached to —N═C═N—. The peaks at 2238 and 2182 cm^{-1} have been observed previously by several groups in amorphous carbon doped with hydrogen and nitrogen.[7,9–11] Our assignment is consistent with those groups. However, this is the first identification of F—N═C═N— mode in *a*-C:H,N,F film.

D. Band in the 1500–1750 cm^{-1} region

As for the band in the 1500–1750 cm^{-1} region, all samples except film *A* have this band, indicating it to be nitrogen related. In this region, nitrogen-activated C-C modes and C-N-related modes can be present. So we fitted this region with four Gaussians with peaks at 1527±5, 1583±1, 1646±8, and 1694±5 cm^{-1}. Figure 4 shows the fitted curves for samples *B*, *C*, and *D*. We assigned the peak

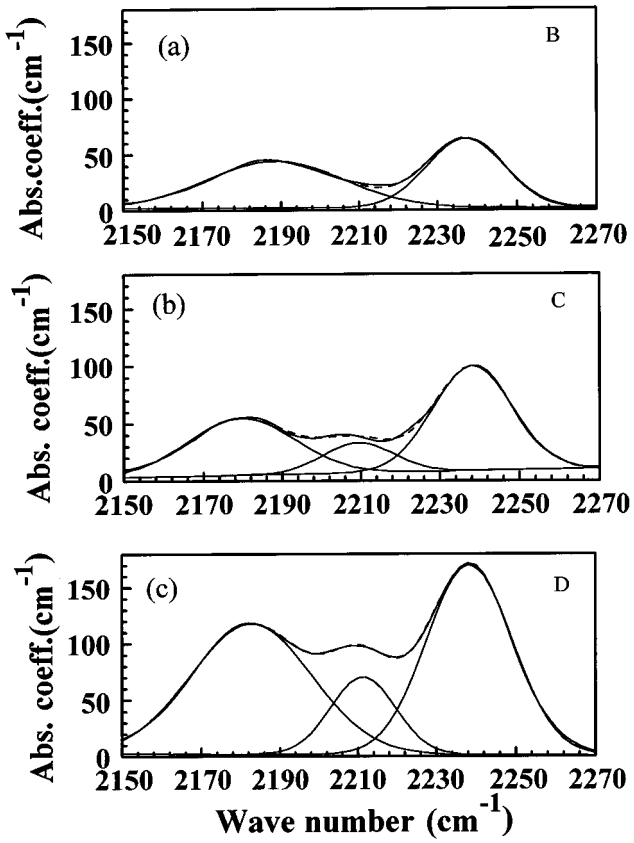

FIG. 3. IR absorption spectra and their fitted curves for the band near 2200 cm^{-1}. The solid lines are fitted curves and the dotted lines are raw spectra. (a) for sample B, the peak positions are at 2188 and 2237 cm^{-1}; (b) for sample *C*, the peak positions are at 2180, 2209, and 2238 cm^{-1}; (c) for sample *D*, the peak positions are at 2182, 2211, and 2238 cm^{-1}.

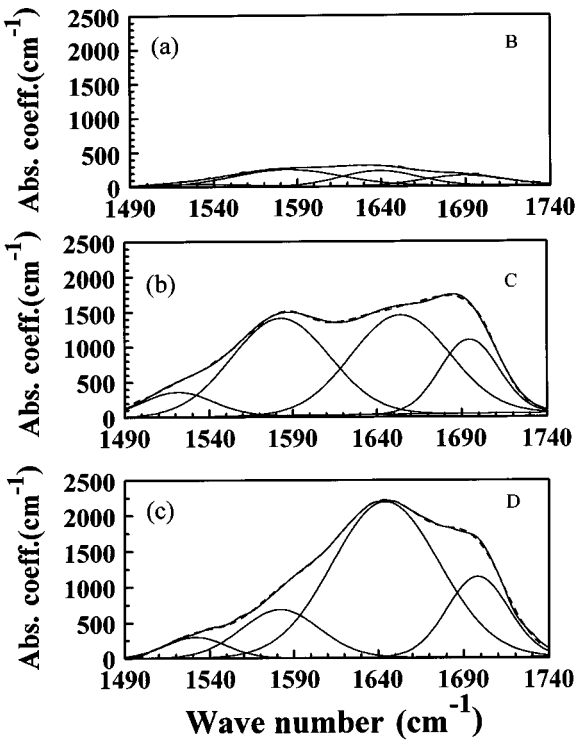

FIG. 4. IR absorption spectra and their fitted curves for the band in the 1490–1740 cm^{-1} region. The solid lines are fitted curves and the dotted lines are raw spectra. (a) For sample *B*, the peak positions are at 1528, 1583, 1639, and 1689 cm^{-1}; (b) for sample *C*, the peak positions are at 1521, 1583, 1654, and 1694 cm^{-1}; (c) for sample *D*, the peak positions are at 1531, 1582, 1644, and 1698 cm^{-1}.

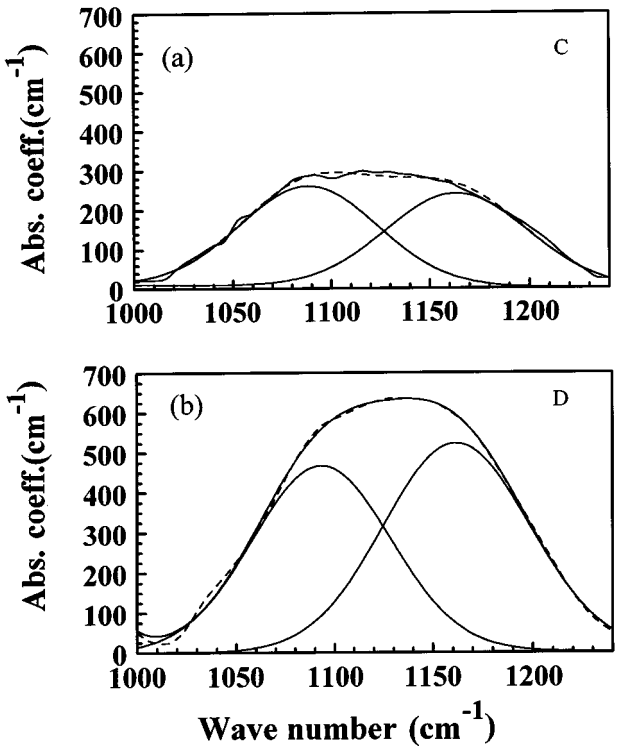

FIG. 5. IR absorption spectra and their fitted curves for the band in the 1000–1240 cm^{-1} region. The solid lines are fitted curves and the dotted lines are raw spectra. (a) For sample *C*, the peak positions are at 1090 and 1164 cm^{-1}; (b) for sample *D*, the peak positions are at 1093 and 1161 cm^{-1}.

at 1694 cm^{-1} to C═N stretch. Usually C═N stretching frequency occurs in the range 1650–1680 cm^{-1}.[19] When one or more NH groups are attached to the carbon atom of the C═N link, the frequencies appear to be slightly higher than usual.[20] The peak at 1646 cm^{-1} can be attributed to the olefinic C═C stretch.[20] This peak becomes IR active because of symmetry breaking by nitrogen doping.[11]

Most primary amines have a NH_2 deformation band in the 1590–1650 cm^{-1} region.[17] We assign the peak at 1583 cm^{-1} to the NH_2 deformation mode.[17] The absolute intensity of this peak decreases in the order of samples *C*, *D*, and *B*. This is consistent with the analysis of the NH_2 stretching mode. The aromatic sp^2 C-C stretch also occurs in this region (1575 cm^{-1}).[16] However, we believe that the peak at 1583 cm^{-1} is not due to aromatic sp^2 C-C stretch for the following reason. If the 1583 cm^{-1} band was from aromatic sp^2 C-C stretch, one should observe the aromatic sp^2 CH stretch at 3050 cm^{-1}. The peak at 3050 cm^{-1} is not present in our spectra. So the assignment of the peak at 1583 cm^{-1} to aromatic sp^2 C-C stretch is unlikely. However, the possibility of its presence in small concentration cannot be excluded. The assignment of the peak at 1527 cm^{-1} is not clear. It might be due to CNH bending.[18] It also follows the trend of NH_2 deformation.

E. Bands in the 500–1250 cm^{-1} region

This region has no peaks for films *A* and *B*. However, when NF_3 is added to CH_4 (films *C* and *D*), three absorption bands show up, indicating that they are C-F or N-F related modes. The band at 1100 cm^{-1} can be fitted with two Gaussians with peaks at 1090 and 1161 cm^{-1}, respectively. Their fitted curves are shown in Fig. 5. Bellamy[19] states that in simple molecules the presence of a single fluorine atom attached to carbon usually results in the appearance of a moderately intense absorption in the 1000–1100 cm^{-1} region. This frequency shifts to higher wave number with further fluorine substitution and splits into two peaks arising from symmetric and asymmetric vibrations. We believe that the peaks at 1090 and 1161 cm^{-1} resulted from the asymmetric and symmetric stretch of bent CF_2, respectively. We calculated a force constant $F_{C—F}=5.94$ mdyn Å and an angle 77.3° between two *C—F* bonds. The asymmetric and symmetric stretching frequencies for bent CF_2 listed in the literature[21] are 1114 and 1225 cm^{-1}, respectively. The calculated force constant and bond angle are $F_{C—P}=5.94$ mdyn Å and $\alpha=81.1°$. It can be seen that there is less than a 4° difference in α between these two cases. The distortion of the bond angle is possible because of the environment around CF_2 and the amorphous nature of the carbon film. The band at 960 cm^{-1} is due to the bent NF_2 asymmetric stretch.[21] The band at 730 cm^{-1} is probably from a C-F deformation mode.[22] Comparing samples *C* and *D*, one can see that the absorption of C-F related peaks for sample *C* is much smaller than that of sample *D*. This can be attributed to the nitrogen dilution of the precursor gases for sample *C*.

In the previous studies of these films on thermal stability of electrical conductivity,[7] it was found that *a*-C:H film (sample *A*) was thermally unstable above 200 °C. Incorporation of fluorine and nitrogen in *a*-C:H (sample *D*) makes the film thermally stable up to 400 °C. From the analysis of IR spectra, we believed that the improvement of thermal stability is probably due to the replacement of weakly bonded C-H in *a*-C:H by strong bonded C-F in *a*-C:H,N,F film.

IV. CONCLUSIONS

We have studied the IR absorption of *a*-C:H and its alloys. IR spectra are analyzed in detail and the peak position assignments are based on the data published in the literature and calculation of the normal mode vibrational frequencies by assuming a simple force field and linear-molecular model. We assigned the absorption peak at 2211 cm^{-1} to in-phase stretching mode of F—N═C═N. We also examined the effects of nitrogen and fluorine on the composition of the carbon films. It was found from the analysis of the CH stretching mode in the 3000 cm^{-1} region that as the concentration of nitrogen and fluorine increases, the ratio of sp^2/sp^3 increases, while the hydrogen concentration decreases. When N_2 is incorporated into carbon films, olefinic C═C stretching mode becomes IR active due to symmetry breaking. When NF_3 is introduced in the precursor gas, C-F related modes show strong absorption indicating significant amount of fluorine incorporation in the carbon film, thus stabilizing the thermal stability of electrical conductivity.

ACKNOWLEDGMENTS

We would like to thank Mark Holtz and Tim Dallas for many helpful discussions. This work was supported in part by the Texas Advanced Technology Program under Contract No. 003644-181, Texas Instruments, and the National Science Foundation under Contract No. Ecs-95-22129.

[1] S. W. Pang and M. W. Horn, IEEE Electron Device Lett. **11**, 391 (1990).
[2] T. E. Derry, R. A. Spits, and J. P. F. Sellschop, Mater. Sci. Eng. B **11**, 249 (1992).
[3] B. Meyerson and F. W. Smith, Solid State Commun. **34**, 531 (1980).
[4] D. I. Jones and A. D. Stewart, Philos. Mag. B **46**, 423 (1982).
[5] Y. Hamakawa, D. Kruangam, M. Deguchi, Y. Hattori, T. Toyama, and H. Okamoto, Appl. Surf. Sci. **33&34**, 1276 (1988).
[6] Y. Hamakawa, T. Toyama, and H. Okamoto, J. Non-Cryst. Solids **115**, 180 (1989).
[7] S. S. Ang, G. Sreenivas, W. D. Brown, H. A. Naseem, and R. K. Ulrich, J. Electron. Mater. **22**, 347 (1993).
[8] G. Sreenivas, S. S. Ang, and W. D. Brown, J. Electron. Mater. **23**, 569 (1994).
[9] He-Xiang Han and Bernard J. Feldman, Solid State Commun. **65**, 921 (1988).
[10] Nobuki Mutsukura, Shin-ichi Inoue, and Yoshio Machi, J. Appl. Phys. **72**, 43 (1992).
[11] J. H. Kaufman, S. Metin, and D. D. Saperstein, Phys. Rev. B **39**, 13 053 (1989).
[12] H. Shanks, C. J. Fang, L. Ley, M. Cardona, F. J. Demond, and S. Kalbitzer, Phys. Status Solidi B **100**, 43 (1980).
[13] K. Mui, D. K. Basa, F. W. Smith, and Reed Corderman, Phys. Rev. B **35**, 8089 (1987).
[14] J. Tauc, R. Grigorovici, and A. Vancu, Phys. Status Solidi **15**, 627 (1966).
[15] J. C. Angus, P. Koidl, and Stanley Domitz, in *Plasma Deposited Thin Films*, edited by J. Mort and F. Jansen (CRC, Boca Raton, FL, 1986), p. 113.
[16] John Robertson, Prog. Solid State Chem. **21**, 199 (1991).
[17] N. B. Colthup, C. H. Daly, and S. E. Wilberly, *Introduction to Infrared and Raman Spectroscopy*, 3rd ed. (Academic, New York, 1990).
[18] H. Siebert, *Anwendungen der Schwingungsspektroskopie in der Anorganischen Chemie* (Springer, Berlin, 1966).
[19] L. J. Bellamy, *The Infra-red Spectra of Complex Molecules* (Chapman and Hall, London, 1975), Vol. 1.
[20] Kiyoshi Ogata, José Fernando Diniz Chubaci, and Fuminori Fujimoto, J. Appl. Phys. **76**, 3791 (1994).
[21] *CRC Handbook of Chemistry and Physics*, 74th ed., edited by David R. Lide (CRC, Boca Raton, FL, 1993), Vol. 9, p. 147.
[22] L. J. Bellamy and R. F. Branch, Nature **173**, 633 (1954).